Appeared in: IEEE Trans. on Instrumentation and Measurement, Vol. 65, No. 9, pp. 2023-2034.

Digital Object Identifier of the paper: 10.1109/TIM.2016.2566818

Appeared in: IEEE Trans. on Instrumentation and Measurement, Vol. 65, No. 9, pp. 2023-2034.

Analysis of the distortion of marker based optical position measurement as a function of exposure time

Tamás Dabóczi, *Senior member*, IEEE
Dept. of Measurement and Information Systems,
Budapest University of Technology and Economics
Budapest, Hungary
daboczi@mit.bme.hu

***Abstract*—Marker based optical position measurement is investigated in this paper. If the exposure time is not very short it might cause the blur of the marker on the image if fast movement needs to be recorded. This study investigates the effect of blur on the center point estimate and provides a measure for the distortion to help adjust camera parameters (exposure time, aperture, ISO sensitivity) in the case of poor lighting conditions. The distortion of the center point estimate is derived as a function of movement of the marker. It is shown that the distortion can be well modeled as integral mean of the marker center. Its distortion can be calculated, and either kept on a limited level by appropriate setting of camera parameters (measure of error is derived), or numerically compensated (inverse filtered). Simulation and measurement examples show the usefulness of the correction.**

Index terms—motion analysis, marker based motion analysis, inverse filtering, deconvolution.

I. INTRODUCTION

Position and orientation measurements are required in many fields of engineering, like motion analysis in sport or medical diagnosis [1][2], robot control [3], analysis of mechanical structures [4] etc. One of the aims of the measurement is to determine the position of a specific point of a body in the 2D (two dimensional) plane or 3D (three dimensional) space, relative to a fixed coordinate system, or relative to the initial position.

Orientation measurement means determining the angle of a segment of the body, again relative to a fixed coordinate system, or relative to the initial orientation.

If human motion is tracked, Inertial Measurement Units (IMU) are widely used to measure the orientation, as they provide much freedom for movement, and occlusion is not a problem. The drawback of the system is that neither of the sensors of the IMU (accelerometer, gyroscope, magnetometer) can precisely measure the orientation. Accelerometer suffers from parasitic forces caused by the movement of the tracked body. (These forces are independent on the angle to be tracked.) Gyroscope signal needs to be integrated, thus even a small bias of the sensor causes an ever increasing error. Magnetometer is unreliable in indoor applications as every metal object distorts the magnetic field of earth. Sensor fusion provides an estimate of the orientation based on the above sensors.

Marker based optical measurement is advantageous for several reasons. It provides both position and orientation measurement. Passive or active markers are placed on the body to be tracked, and the motion is recorded by several cameras [5]. Positions of the markers are determined from the individual frames. If 3D reconstruction is required, triangulation is also performed based on different camera measurements. Orientation is determined from the positions of markers on the same segment of the body. Marker based orientation measurement can also be a validation technique for development of sensor fusion algorithm for IMU. The drawback is that repeatability of the measurement depends strongly on how precisely the markers can be placed on the same location of the body. In human motion analysis one of the problems is that the skin can slightly shift relative to the anatomical landmark point. The dependence and possible correction of the error is discussed in [6].

Novel techniques determine the position without placing special markers on the body (marker-less motion capture) just by determining feature points on the image [7] or analyzing the texture [8]. Others combine marker-less motion capture with IMU measurement [9]. These techniques are computationally very intensive,

which is anyhow a drawback of optical measurements. Moreover, position measurement is not possible in the case of occlusion, although there are systems utilizing more than 20 cameras. There are also attempts to estimate the trajectory of the motion in the case of partial occlusion, illumination variation and motion blur with the help of principal component analysis [10].

Many times position measurement is not the final goal of the investigation; other features are derived from this primary measurement, like speed, acceleration of the body, or rotational speed, rotational acceleration of segments. Often a body or frame model with rigid segments coupled with joints is assumed, and model parameters are fitted to the observations [11][12].

In this study, marker based position measurement is investigated from the point of view of motion blur caused by the (relative) large exposure time. As company Robert Bosch notes [13], motion blur is one of the most serious error sources of CCTV based measurements because of the relatively slow shutter speed. E.g. in automotive applications lighting conditions may vary between extreme values, and – as the car may move fast – objects to be detected might easily be blurred (e.g. feature points of a scene to identify lane, obstacles, pedestrians, traffic signs etc.). We face the problem in many other fields that lighting conditions cannot be influenced, fast motion needs to be tracked and ambient light provide poor measurement. There are many techniques to determine and remove the motion blur of the camera, or the blur of just an object within the image (e.g. [14]). These algorithms are rather complex, require much computation. Our aim is not to recover the original sharp image, just to extract a specific feature of the marker, namely its position. Much larger blur is tolerable if only this feature needs to be extracted. This paper provides a measure for the distortion for the case of weighted geometric centroid based center point estimate. It allows an objective means to determine optimal camera settings (exposure time, aperture, ISO sensitivity) based on lighting conditions and frequency of movement of the object. It will be shown that the distortion can be numerically compensated (inverse filtered), or under certain circumstances even avoided. It will also be shown that avoiding significant distortion does not require setting the exposure to a very short time (and thus freezing the frame). Even a moderate

exposure time can provide good position estimate, although the marker images are blurred. Increasing the exposure time allows us to improve the signal to noise ratio of the measurement. The user has the freedom either to eliminate the distortion on the price of slight SNR reduction, or to compensate it by means of inverse filtering. The analysis also helps to decide whether a commercial camera is enough for the purposes, or a semi-professional camera or high-end (and expansive) motion analysis setup is required to avoid motion blur. It also supports the design of required measurement setup by providing a measure for the decision whether ambient light provide enough signal-to-noise ratio or lighting conditions need to be influenced (e.g. additional light source or active marker).

The paper is organized as follows. Section II collects the most frequent methods to estimate marker position of video based measurements. Section III deals with the effect of motion blur of marker image on the center point estimate of geometric centroid based method, and proposes an easy method to compensate its distortion by means of inverse filtering. Section IV validates the concept on measurement example. Appendix provides a detailed derivation of the effect of time domain trajectory of the marker on the intensity distribution of individual pixels, and on the center point estimate of the marker.

II. MARKER BASED OPTICAL POSITION MEASUREMENT

The body of the investigated object is equipped with markers apart from each other. Usually markers that produce circular images are used. A camera records the movement of the object. After some signal enhancement and nonlinear filtering the marker can be roughly localized on the individual frames. Preprocessing might include noise filtering, selection the region of interest, color based filtering, edge detection etc. The next step is to find the center point of the marker images. Orientation (if required) can be determined from the angle of the line across the center points of different markers. This paper focuses on the center point estimate and the effect of slow shutter speed on it. If the movement during the exposure is not negligible, the image of the marker is a blurred version of a circle. We determine the effect of motion blur on the center point

estimate and provide compensation. Throughout the paper I will assume that motion blur and other linear distortions will dominate, and the analysis do not cover the effect of non-linear distortion of the lens on the center point estimate.

A. Center point estimates

The image can be considered as a plane body with uniform or non-uniform weight distribution. Center point estimation is analogous to find the center of gravity of the body, thus in the following we will use the terms center point and center of gravity interchangeably. Uniform weight distribution corresponds to binary images for which covered marker pixels are derived by thresholding. This was the case in early motion analyzers where the hardware and the online processing capability did not allow processing of intensity data. Non-uniform weight distribution corresponds to intensity information, which might be either a gray scale image, or a particular color of the 3-channel color image. The latter is advantageous if the color of the marker can be well separated from the remaining part of the image. This technique includes utilizing red LEDs, or passive markers reflecting infrared light, and optically filtering IR color.

The most popular center point estimates are the calculation of the geometric centroid, circle fitting and fitting Gaussian marker model. A more sophisticated method is the BEWRI (Best Estimation Without Radius Information).

1) Geometric centroid

The center of gravity of a body having a distributed weight in a 2D plane can be calculated as follows:

$$\underline{r}_{cog} = \frac{1}{M}\int_A \underline{r}\,\rho(\underline{r})dA\,; \qquad M = \int_A \rho(\underline{r})dA \tag{1}$$

where $\underline{r}_{cog}$ is the vector of center of gravity, $\rho(\underline{r})$ describes the weight distribution (weight density function) and M is the total mass of the body. If the marker image is binary (covered and uncovered pixels) and we

assume uniform intensity distribution (same gray scale value for all covered pixels), the center estimate of the marker can be calculated from the coordinates of the covered pixels:

$$x_{cog} = \frac{1}{N}\sum_{i=1}^{N} x_i \ ; \qquad y_{cog} = \frac{1}{N}\sum_{i=1}^{N} y_i \tag{2}$$

where x_i and y_i are the coordinates of the covered pixels, x_{cog} and y_{cog} are the estimated coordinates of the marker center. If the algorithm is implemented for real-time processing it is advantageous to start the computation immediately as a covered pixel is detected. For that a modified calculation can work on scan lines

$$x_{cog} = \frac{\sum_{i=1}^{L}\left(x_{end,i} - \frac{d_i}{2}\right) d_i}{\sum_{i=1}^{L} d_i} \ ; \qquad y_{cog} = \frac{\sum_{i=1}^{L} y_i d_i}{\sum_{i=1}^{L} d_i} \tag{3}$$

where L is the number of scan lines, d_i is the width of the covered marker image in the *i*-th row, $x_{end,i}$ denotes the last *x* coordinate of the covered marker in the *i*-th row, and y_i denotes the *y* coordinate of the *i*-th row.

2) Circle fitting

More computation is required if a circle is fitted to the contour line of the marker image. If the radius of the marker image is assumed to be known (*R*), the following error function needs to be minimized with respect to x_{cog} and y_{cog}:

$$\sum_i \left(\sqrt{\left(x_{cog} - x_{cont,i}\right)^2 + \left(y_{cog} - y_{cont,i}\right)^2} - R\right)^2 \tag{4}$$

Geometry of the CCD has to be taken into account. (In some cameras the elementary pixel size is not the same in the two directions. In that case the coordinates need to be scaled.) Usually a modified error function is optimized instead of the traditional least squares fit to speed up the inherently nonlinear procedure:

$$\sum_i \left(\left(x_{cog} - x_{cont,i}\right)^2 + \left(y_{cog} - y_{cont,i}\right)^2 - R^2 \right)^2 \tag{5}$$

3) Fitting Gaussian marker model

In [12] Gaussian marker model is used to describe the partial coverage of the pixel by the marker. The intensity distribution is assumed to be:

$$I(r) = A\, e^{\left(-(r-x_c)^2/(2\sigma^2)\right)} \tag{6}$$

The parameters of the distribution are fitted to the measurement.

4) Best Estimation Without Radius Information (BEWRI)

This algorithm - developed by Á. Jobbágy [15][16] - eliminates the need of a priori information about the radius of marker image. The required steps are the following:

1. Compute the minimal (r_{min}) and maximal radius (r_{max}) that can cover the pixels of marker image
2. To r_{min} determine the corresponding area (A_{min}) so that a disk with radius r_{min} and center point anywhere along A_{min} results in the marker image. For A_{min} calculate the center of gravity (CG_{min}).
3. Repeat the previous step for $r_i = r_{min} + \Delta\, r$ until it reaches r_{max}. Let us denote the calculated parameters by A_i and CG_i.
4. The center of gravity estimate is considered as the weighted average of the set of CG_i:

$$CG = \frac{\sum_i A_i CG_i}{\sum_i A_i}$$

III. CENTER POINT ESTIMATE ON BLURRED IMAGE

Moving marker causes a blurred image if the shutter speed of the CCD is slow. The blur is proportional to the speed of the motion along the image plane. The image of the marker is not a circle anymore; it becomes a

trail of light. We are interested in the position of the marker at a specific time instance. (E.g. at the middle of exposure. On that way the time window of the exposure is symmetric to the sample instance.) It is obvious that coordinates of the center point at the middle of exposure will usually differ from the estimates of center points based on the blurred marker image (see Fig. 1.). The amount of effect might be different but all center point estimates will fail if the trajectory of movement is not symmetric to the middle time of the exposure.

In the next subsection it will be shown that the effect of motion blur of marker images on geometric centroid estimate can be mathematically described and systematically compensated. It should be noted that we are not interested in removing the motion blur, i.e. reconstructing the original still image. Our primary aim is only to avoid or correct the error of the center point estimate.

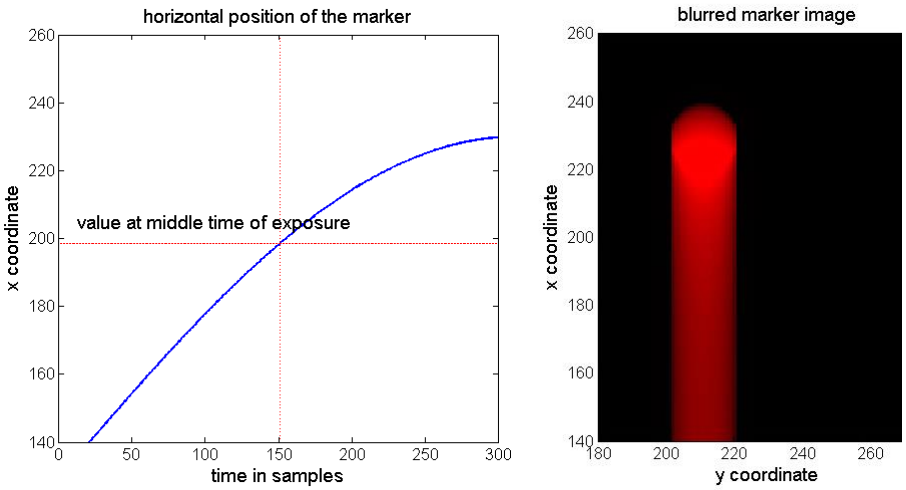

Fig. 1. Visualization of the blurred marker image (simulated image)

A. Marker has negligible dimension

First let us assume that the marker can be modeled as a point light source (one pixel only). The marker image at a particular time is a gray scale picture. For the sake of simplicity of derivation we will assume a motion along only the *x* axis in the image plane. As all operations are linear, the results remain valid for arbitrary motion based on the superposition. We will also assume that the marker movement is bandlimited, and the

sampling theorem is fulfilled. Thus, the trajectory of the marker can be considered as the superposition of sinusoidal movements. From the point of view of marker movement the sampling frequency is the frame rate.

Center of gravity can be calculated as:

$$x_{cog} = \frac{\int_{x_{min}}^{x_{max}} x\, \rho(x) dx}{\int_{x_{min}}^{x_{max}} \rho(x) dx}\ , \tag{7}$$

where $\rho(x)$ denotes weight density function, x_{min} and x_{max} denote the coordinates of the body border. Replacing the weight distribution with the intensity distribution (brightness) of the image we get the geometric centroid based center point estimate. Intensity distribution or gray scale distribution is described by intensity density function, which means the brightness of a small interval or area, in discrete case the brightness of one pixel:

$$x_{cog} = \frac{\int_{x_{min}}^{x_{max}} x\, i(x) dx}{\int_{x_{min}}^{x_{max}} i(x) dx} \tag{8}$$

where $i(x)$ is the intensity density function with respect to *x*. For sampled images the integral becomes a sum:

$$x_{cog} = \frac{\sum_{k=x_{min}}^{x_{max}} k\, i(k)}{\sum_{k=x_{min}}^{x_{max}} i(k)} \tag{9}$$

In the remaining, we will derive the expressions for continuous space and time, but the result is valid for the sampled image, as the intensity of a pixel is simply the integral of the intensity density function for a small area (in 1D case for a section). The denominator in (8) is constant throughout the measurement; it depends on the shutter speed and brightness of the marker:

$$\int_{x_{min}}^{x_{max}} i(x) dx = g(\tau, I_{marker}) \tag{10}$$

where τ denotes the duration of exposure, I_{marker} denotes brightness of the marker and $g(\tau, I_{marker})$ means that the expression is a function of the two variables. The numerator of the center point expression in (8) – which is an integral according to space – can be rewritten as an integral according to time (see derivation in Appendix 1). Thus the center point estimate becomes:

$$x_{cog} = \frac{\frac{1}{\tau}\int_{-\tau/2}^{\tau/2} x_c(t)dt}{g(\tau, I_{marker})} \tag{11}$$

where $x_c(t)$ is the trajectory of the marker center along the x axis. Apart from a constant multiplicator the expression is the integral mean of the time domain signal during the exposure of a single frame. Its distortion is:

$$H(f) = \frac{\sin(\pi f \tau)}{\pi f \tau} \tag{12}$$

where distortion is meant as the decrease of the amplitudes of Fourier components of marker movement. This distortion for different exposure times is shown in Fig. 2. Please note that slight decrease of exposure time can significantly decrease the error of center point estimate. The exposure time does not need to be decreased until the fast movement freezes, i.e. motion blur is less than 1 pixel (e.g. at 5 Hz movement to around 1/2000 sec), it is enough to decrease it to a tolerable blur (in the above example to around 1/250 sec). (Certainly, if lighting conditions allow, it is always better to measure the movement with the smaller exposure.)

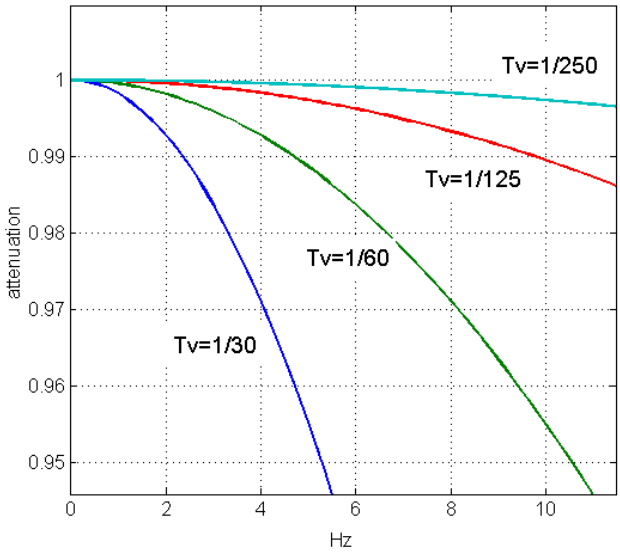

Fig. 2. Effect of finite exposure on the center point estimate. Frequency dependent distortion is depicted for different exposure times (Tv stands for τ, the usual abbreviation of exposure times on cameras). Attenuation means the reduction of observed amplitude for sinusoidal excitation of the marker.

Alternatively, we can increase the exposure time to have a good signal to noise ratio, and inverse filter the center point estimates using the following transfer function:

$$H_{inv}(f) = \begin{cases} \dfrac{\pi f \tau}{\sin(\pi f \tau)} & if\ 0 < f < f_s/2 \\ 1 & if\ f = 0 \end{cases} \tag{13}$$

As the inverse filtering will be accomplished in the digital domain the above function should be mirrored and extended to represent negative frequencies in the DFT. No overlapping of sinc function should be modeled if the requirement of sampling theorem is met by the motion of the marker. Trajectory of the marker does not need to be reconstructed on a very fine time grid to eliminate its blur effect; it is enough to estimate the center points of the marker at time instances of the capture of video frames.

B. Marker has finite dimension

If the marker has finite radius the intensity of the pixels depend not only on the movement but also on the width of the marker. It can be shown that the 2D center point estimate based on weighted averaging is the

weighted superposition of center point estimates along scan lines. If the direction of movement is horizontal (along scan lines), the above weights for the superposition do not depend on the movement, thus it is enough to investigate only one scan line, and derive the distortion for that.

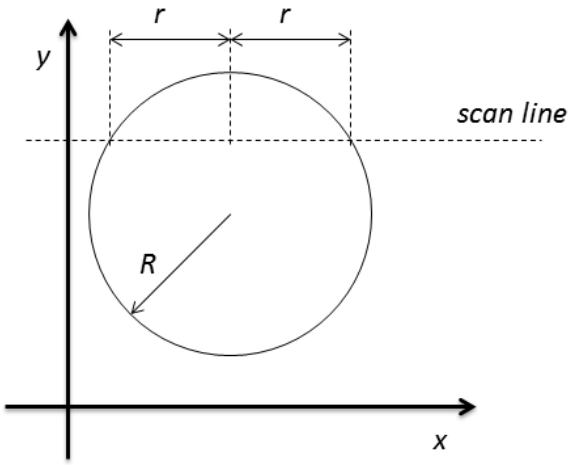

Fig. 3. Marker is investigated along a scan line

The intensity distribution (intensity density function) of the marker image along a scan line becomes (see Appendix 2 for detailed derivation):

$$i(x) = \frac{1}{\tau} \cdot \frac{t^*(x+r) - t^*(x-r)}{2r} \approx \frac{1}{\tau} \frac{dt^*(x)}{dx} \tag{14}$$

where $t(x)$ is the inverse function of the marker movement along the scan line, $x_c(t)$, $2r$ is the width of the marker along the scan line, and $t^*(x)$ is its extension at the borders of the movement:

$$t^*(x) = \begin{cases} -\tau/2 & if\ x < x_{c,min} + r \\ t(x) & if\ x_{c,min} + r < x < x_{c,max} - r \\ +\tau/2 & if\ x_{c,max} - r < x \end{cases} \tag{15}$$

If we compare it with the intensity density function for the case of point like marker:

$$i(x) = \frac{1}{\tau} \frac{dt(x)}{dx} \tag{16}$$

we can conclude that the difference is that derivative is replaced with finite difference. The rest of the derivation of result is the same as that for point like markers. Thus the center point estimate becomes as close to the integral mean (see (11)) as close the finite difference in (14) to the derivative is.

IV. SIMULATION EXAMPLE

In the following, simulations are given concerning the intensity distributions of a marker with finite dimension. The marker is moved along one axis according to a time function. The effect of blur on the CCD can be calculated by dividing the exposure time to very small time instances, and assuming that the blur will be the superposition of intensity distributions of still marker images sampled at a fine time grid.

A. Sinusoidal movement; marker has finite dimension

First the marker is moved according to a sinusoidal function, with different frequencies, and the marker center is estimated on every frame with weighted geometric centroid. The radius of the marker is 10 pixels, which is 10% of the amplitude of movement. Frame rate is 25 fps, simulated time of exposure is 1/30 s. The decrease of the amplitude is compared with the theoretical one, assuming point like marker described in (12). A sine wave is fitted to the estimated center points with four parameter sine fitting algorithm [17]. The error of the amplitude measurement together with the theoretical one is depicted in Fig. 4. The two curves are the same, within graphic resolution (max. relative error is 10^{-3}). According to simulations the deviation from the ideal curve remains the same for a very broad range of marker size (marker size from 10% up to 400% of the amplitude of the movement has been checked). The standard deviation of the fit at different frequencies is shown in Fig. 5. (Center point estimate along the other axis has negligible error, as there is no movement in that direction.) This shows that the theoretical distortion derived for point like marker can be well used for markers with finite dimension.

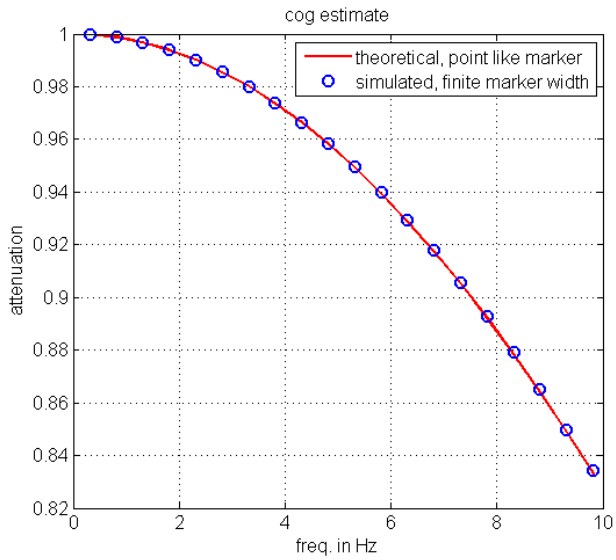

Fig. 4. Effect of motion blur on center point estimate: magnitude of the transfer function (25 fps, 1/30 s exposure). Red line: theoretical distortion if marker is point like; blue circles: simulated, if marker has finite dimension (they are nearly the same within graphical resolution). Attenuation means the reduction of observed amplitude for sinusoidal excitation of the marker.

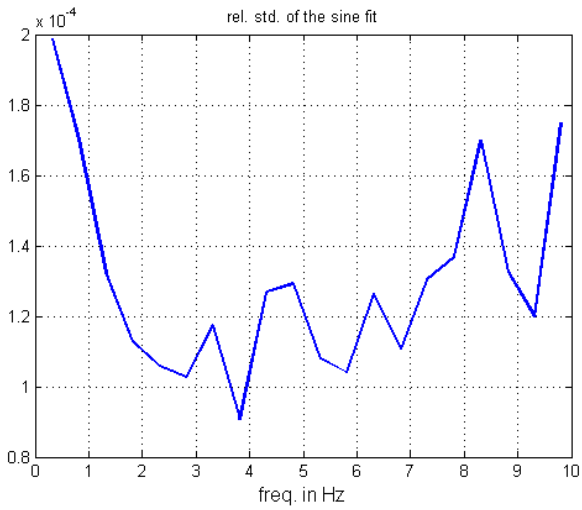

Fig. 5. Relative root mean squares error of the sine fit of center point estimates. Marker radius: 10% of sine amplitude. Error is defined as the difference between the coordinates of marker center estimate and sine fit.

B. Compensation of the distortion for a complex waveform; marker has finite dimension

Let us check the possibility of correcting the distortion for a more complex waveform. An aperiodic function is simulated with four sine waves, having mutually irrational frequency ratios (f_1=0.543 Hz; f_2=2.112 Hz;

f_3=3.522 Hz; f_4=5.444 Hz), see Fig. 6. Noise source is the quantization noise (8 bit color depth for gray scale image).

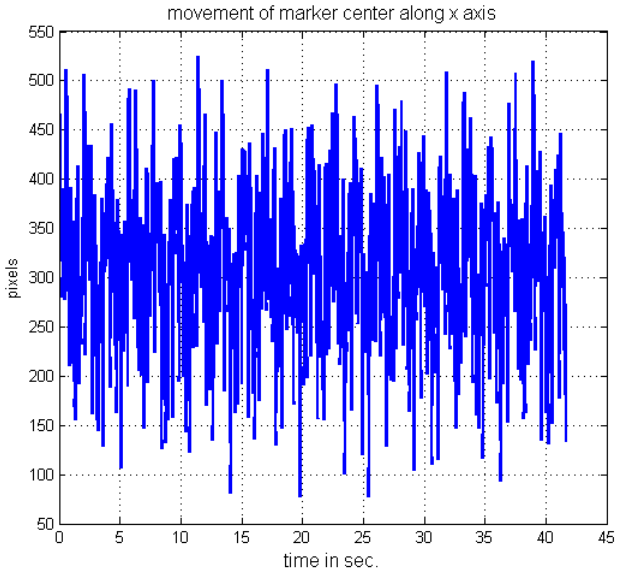

Fig. 6. Time function of the movement of marker along x axis

The distortion of the center point estimate is compensated with (13), having an impulse response depicted in Fig. 7. The inverse filtered center point estimate is very close to the true one, the two cannot be distinguished on a plot; thus the difference is depicted in Fig. 8. The error is decreased by a factor of 100, apart from the transient of the inverse filter at the beginning of the record. (Here error is defined as the difference between the coordinates of marker center estimate and true location of marker center.) It should be noted that the motion blur of the image is not removed, just its effect on the center point estimate.

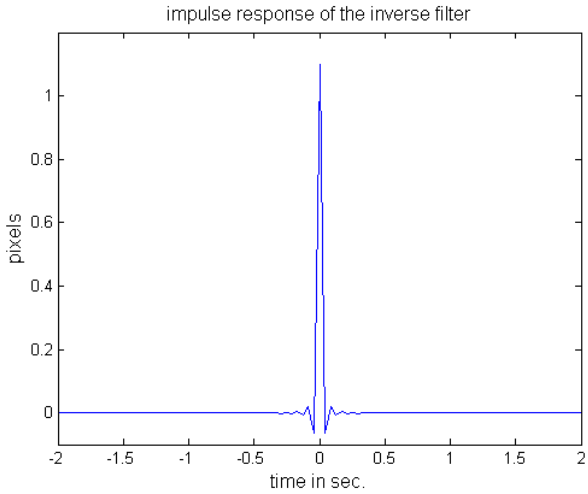

Fig. 7. Impulse response of the inverse filter

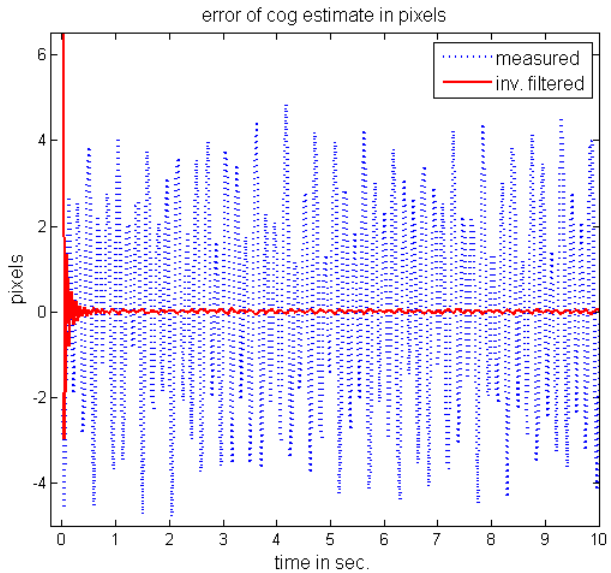

Fig. 8. Error of the center point estimate: based on measured cog (dotted line), based on inverse filtered cog (solid line)

V. MEASUREMENT EXAMPLE

Our aim is to measure the transfer function caused by the relative large exposure. For system identification either we need to move a marker according to a well-defined trajectory (provide a well-defined excitation signal), or we need a reference measurement device (measure the excitation signal). We chose the first approach. If the marker is put on a plate, which is rotated with constant speed around the vertical axis, the

trajectory of the marker along the horizontal axis is a sinusoidal function. We may control the rotational speed, and can measure the amplitude. The transfer function is measured on this way step-by-step at different frequencies. Attenuation is defined as the decrease of the amplitude of the sine wave. (Phase shift will not be investigated.) We need to measure the amplitude of the recorded trajectory of center points on the best way. A camera is placed far enough from the marker to see its movement from a narrow angle, thus change of distance and (projected) size of the marker is negligible. Cameras viewing axis is perpendicular to the rotation angle, thus the marker moves approximately along horizontal scan lines on the image. (The horizon of the camera was not precisely aligned to the plane of the movement, thus motion not along scan lines is also demonstrated.) The measurement setup is shown in Fig. 9. A semi-professional DSLR camera (Canon EOS 700D) was used to record the movement. In this experiment the distance was 3 m, and the lens used to cover the distance and viewing angle was a zoom lens having a maximal focal length of 320 mm. The shooting parameters can be freely adjusted on that camera, even for movie recording. First 1/30 s exposure time has been selected with aperture value of 5.6, frame rate of 25 fps at different ISO speeds. This measurement has been compared to the one with a slight decrease of the exposure time (1/125). The recording was remotely controlled to eliminate any shake by starting and stopping the recording. The experiment has been carried out with different markers, both passive and active ones. The best performance has been achieved in a dark room with a LED as a marker. The motor rotating the plate was a stepper motor with 200 steps/rotation, and 1600 micro steps/rotation. We used micro stepping. The impulses for the micro stepping were generated by a microcontroller, having a timer with timing precision of ordinary quartz (~10 ppm).

A movie of ~20 sec. was recorded, and separated off-line to individual frames. Image processing consisted of the following steps. First the region of interest has been (manually) selected to get rid of those parts of the pictures where the marker cannot appear. The next step was a color filtering to emphasize the specific hue of the marker (in this case selection of green channel as the marker was a green LED), followed by adaptive thresholding. At the first step 10% of the maximal intensity of green channel of individual frames has been

selected as threshold. The weighted geometric centroid was calculated on that image to get an estimate about the center of the marker. During this system identification phase we can make use the fact that the excitation signal is sinusoid. Our assumption (supported by theoretical derivation) is that the system is linear. Thus, the system response is restricted to be a sine wave as well. Four parameter sine fitting algorithm was applied to the center point estimates. The aim of sine fitting is to measure the amplitude, and on that way the attenuation at individual frequencies. The signal to noise ratio of the attenuation measurement can be improved, if the whole procedure is repeated with a narrower region of interest around the measured center points, or around the fitted sine wave (we do not correct the trajectory, just the region of interest for noise reduction is selected). Thresholding was omitted in the refinement step. The time function of the center point of the marker is calculated again, and finally a sine wave is fitted to the center point estimates to determine the parameters of the movement (Fig. 10), and extract attenuation information at the specific frequency. The measurement has been repeated for several frequencies to scan the transfer function in the frequency band of interest. All calculations were carried out off-line in Matlab (for validating the results, there is no real-time requirement).

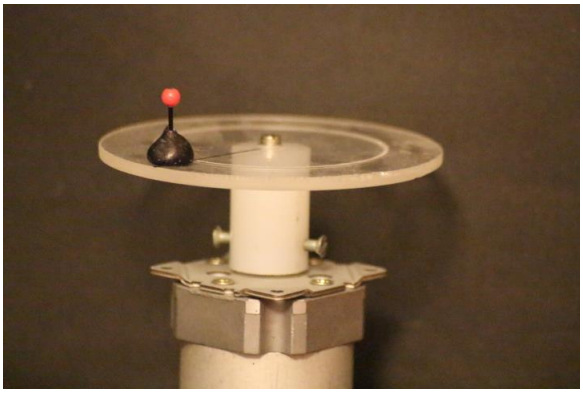

Fig. 9. Measurement setup to produce a well-defined marker movement

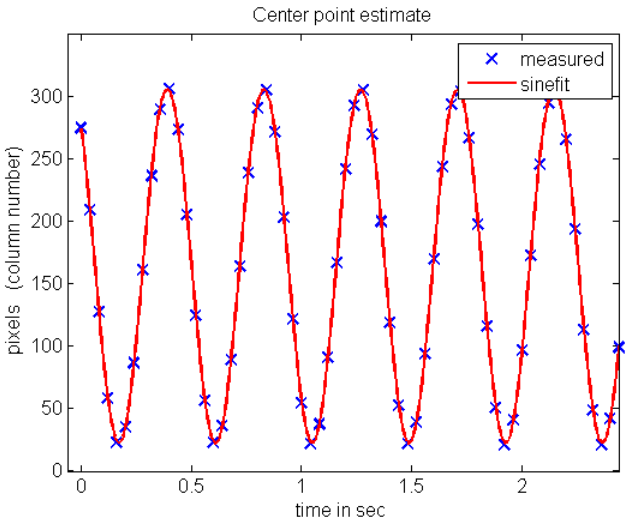

Fig. 10. Center point estimate and the fitted sine wave. f=2.5 Hz, Tv=1/30, ISO 6400.

The amplitude of the sine wave based on the estimate of the blurred image at Tv=1/30 s is 141.0 pixels, compared to 144.4 that was measured at very slow speed (no motion blur), which corresponds to an attenuation of 0.977. The attenuations at different frequencies and at different CCD sensitivities (ISO speeds) compared to that of theoretical one with point like markers are depicted in Fig. 11. At small frequencies the shape of the attenuation is the same as the theoretical one with finite marker width. At large frequencies and low sensitivity (low ISO speed) the intensity of the individual pixels becomes low as the blur increases, causing an increasing uncertainty of the center point estimate and the sine fit. The fit is unstable above 2.5 Hz at ISO 1600, and above 2 Hz at ISO 200. An additional attenuation can be observed by the measurements at ISO 1600 and ISO 6400. The difference comes from the fact that above ISO 400 sensitivity several pixels saturate at around the peak of the sine wave, which distort the weighted center point estimate. Measurement at ISO 200, Tv=1/30 s did not show saturation, and the measurement follows well the theoretical curve until it becomes unstable because of the bad SNR.

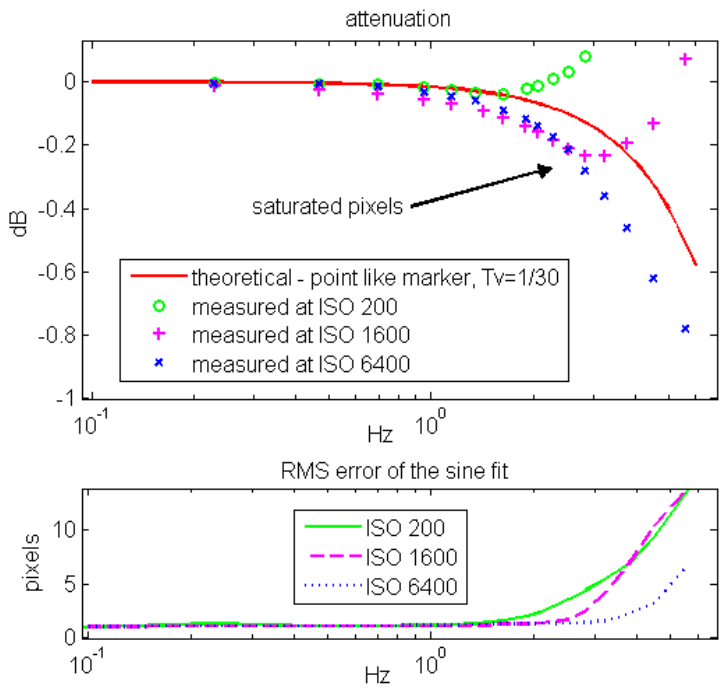

Fig. 11. Attenuation of the center point estimate at different CCD sensitivities, together with the uncertainty of the sine fit. Tv=1/30. Above ISO200 the pixel intensity saturates, causing an additional distortion. Attenuation means the reduction of observed amplitude for sinusoidal excitation of the marker.

By investigating Fig. 2 we can conclude that slight decrease of exposure time might decrease the error significantly. Thus, the measurement has been repeated for Tv=1/125 s, for which the image is still blurred (compare Fig. 12 with Fig. 13), but center point estimate is much more accurate. The ISO sensitivity is increased to 800, which corresponds to the same sensitivity as Tv=1/30 s, ISO 200. The comparison of the attenuations is shown in Fig. 14. Measured attenuation at Tv=1/125 s aligns well with the theoretical value, even though the marker size is larger than one pixel.

Fig. 12. Blur of the active marker at around 200 rpm (3.24 Hz), Tv=1/30 s, ISO 6400, two different samples. Width of the picture corresponds approximately to the range of the movement, i.e. the trail corresponds to ~10% of one circle.

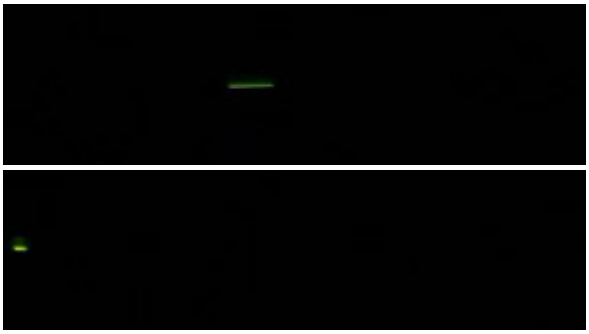

Fig. 13. Blur of the active marker at around 200 rpm (3.24 Hz), Tv=1/125 s, ISO 800, two different samples. Width of the picture corresponds approximately to the range of the movement, i.e. the trail corresponds to ~2.6% of one circle.

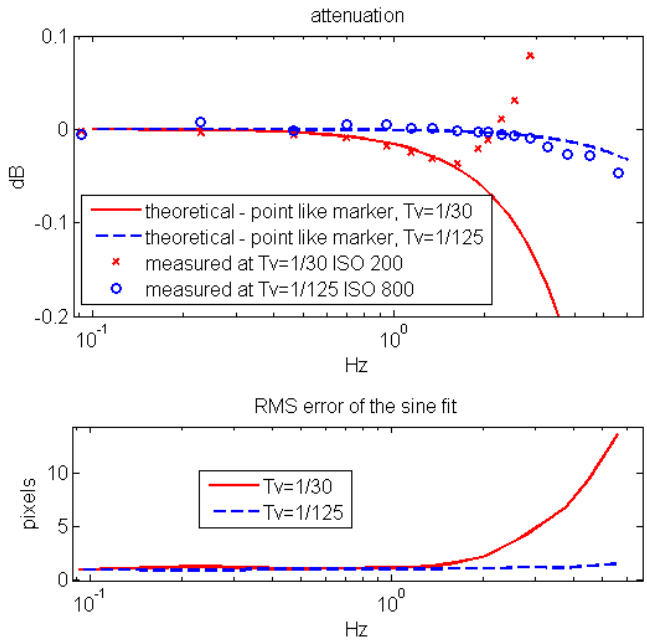

Fig. 14. Attenuation of the amplitude of center point estimate, together with the uncertainty of the sine fit. Theoretical one derived for point like marker: solid line (Tv=1/30 s), dashed line (Tv=1/125 s). Meaured center point attenuation with finite width marker: crosses (Tv=1/30 s), circles (Tv=1/125 s). Attenuation means the reduction of observed amplitude for sinusoidal excitation of the marker.

The conclusion is that the distortion of center point in the case of markers with finite radius can be well calculated based on the theoretical distortion derived for point like light source. However, care should be taken to increase the ISO sensitivity only up to the level for which the pixels do not saturate.

VI. Conclusions

Distortion of marker based position estimate was investigated as a function of exposure time. The distortion of the amplitude of the trajectory of the marker caused by the blurred images were derived theoretically for point like light sources. The effect of finite marker radius was also described and its distortion was approximated. Condition for the approximation was shown. Both simulation and measurement examples support that this model can be well used for markers with finite radius. The analysis helps determine the optimal camera settings in poor lighting conditions. It was shown that motion blur does not need to be removed; it is

enough to keep its effect moderate on marker center point estimate. It was also shown that exposure time does not need to be decreased until images on individual frames freeze. Center point can be well estimated from blurred images. Distortion can be either eliminated or compensated numerically, if required.

ACKNOWLEDGMENT

This work was partially supported by the ARTEMIS JU in the frame of the R5-COP project and the Hungarian National Research, Development and Innovation Fund (OTKA K115820).

REFERENCES

[1] Ryan Janssen, et al., “Active Markers in Operative Motion Analysis,” IEEE TRANSACTIONS ON INSTRUMENTATION AND MEASUREMENT, VOL. 55, NO. 3, JUNE 2006, pp. 854-859.

[2] Joseph E. McNamara et al., “An Assessment of a Low-Cost Visual Tracking System (VTS) to Detect and Compensate for Patient Motion During SPECT,” IEEE TRANSACTIONS ON NUCLEAR SCIENCE, VOL. 55, NO. 3, JUNE 2008, pp. 992- 998.

[3] Young-Keun Kim et al., “Developing Accurate Long-Distance 6-DOF Motion Detection With One-Dimensional Laser Sensors: Three-Beam Detection System,” IEEE TRANSACTIONS ON INDUSTRIAL ELECTRONICS, VOL. 60, NO. 8, AUGUST 2013, pp. 3386- 3395.

[4] Hyo Seon Park, Keunhyoung Park, Yousok Kim, and Se Woon Choi, “Deformation Monitoring of a Building Structure Using a Motion Capture System,” IEEE/ASME TRANSACTIONS ON MECHATRONICS, VOL. 20, NO. 5, OCTOBER 2015, pp. 2276-2284.

[5] Luca De Vito, Octavian Postolache and Sergio Rapuano, “Measurements and Sensors for Motion Tracking in Motor Rehabilitation,” IEEE Instrumentation & Measurement Magazine, June 2014, pp. 30-38.

[6] Roya Haratian, Richard Twycross-Lewis, Tijana Timotijevic, and Chris Phillips, “Toward Flexibility in Sensor Placement for Motion Capture Systems: A Signal Processing Approach,” IEEE SENSORS JOURNAL, VOL. 14, NO. 3, MARCH 2014, pp. 701-709.

[7] Kun Li, Qionghai Dai and Wenli Xu, “Markerless Shape and Motion Capture from Multiview Video Sequences” IEEE TRANSACTIONS ON CIRCUITS AND SYSTEMS FOR VIDEO TECHNOLOGY, VOL. 21, NO. 3, MARCH 2011, pp. 320-334.

[8] Björn Holmberg, Håkan Lanshammar, “Possibilities of texture based motion analysis,” Computer Methods and Programs in Biomedicine, Volume 84, Issue 1, October 2006, pp. 1–10,

[9] Ya Tian, William R. Hamel and Jindong Tan, “Accurate Human Navigation Using Wearable Monocular Visual and Inertial Sensors,” IEEE TRANSACTIONS ON INSTRUMENTATION AND MEASUREMENT, VOL. 63, NO. 1, JANUARY 2014, pp. 203-213.

[10] Haicang Liu, Shutao Li and Leyuan Fang, “Robust Object Tracking Based on Principal Component Analysis and Local Sparse Representation,” IEEE TRANSACTIONS ON INSTRUMENTATION AND MEASUREMENT, VOL. 64, NO. 11, NOVEMBER 2015, pp. 2863-2875.

[11] Paavo Vartiainen, Timo Bragge, Jari P. Arokoski, and Pasi A. Karjalainen, “Nonlinear State-Space Modeling of Human Motion Using 2-D Marker Observations,” IEEE TRANSACTIONS ON BIOMEDICAL ENGINEERING, VOL. 61, NO. 7, JULY 2014, pp. 2167-2178.

[12] Ivo Stancic, Tamara Grujic Supuk, Ante Panjkota, “Design, development and evaluation of optical motion-tracking system based on active white light markers,” IET Science, Measurement and Technology, 2013, Vol. 7, Iss. 4, pp. 206–214.

[13] “Application Note: Use of Dinion^{XF} Cameras to Reduce Motion Blur”, Bosch Security Systems, 2004. Available online at: http://resource.boschsecurity.us/documents/Application_note_enUS_2103511051.pdf. Downloaded 10/13/2015.

[14] Amit Agrawal, Yi Xu and Ramesh Raskar, “Invertible Motion Blur in Video,” ACM Transactions on Graphics, 2009, Vol. 28, No. 3, Article 95, pp. 95:1-95:8.

[15] Jobbagy A, Furnee EH, “Marker Center Estimation Algorithms in CCD Camera-based Motion Analysis,” MEDICAL AND BIOLOGICAL ENGINEERING AND COMPUTING 32:(1) pp. 85-91., 1994.

[16] Ákos Jobbágy and Hans Furnee, “New marker centre estimation algorithm of high accuracy in motion analysis,” PERIODICA POLYTECHNICA SER. EL. ENG. VOL. 36, NOS. 3-4, PP. 249-258 (1992)

[17] Kollar, I.; Blair, Jerome J., “Improved determination of the best fitting sine wave in ADC testing,” IEEE TRANSACTIONS ON INSTRUMENTATION AND MEASUREMENT, VOL. 54, NO. 5, 2005, pp. 1978-1983.

APPENDIX 1 – POINT-LIKE MARKER

Center of gravity (center point of marker based on geometric centroid) can be calculated as follows:

$$x_{cog} = \frac{\int_{x_{min}}^{x_{max}} x\, i(x) dx}{\int_{x_{min}}^{x_{max}} i(x) dx} \tag{17}$$

where $i(x)$ is the intensity density function (gray scale distribution of brightness) with respect to x.

A. Intensity as a function of time instead of space

1) Monotonic function

Let us assume that the marker center moves according to a strictly monotonic increasing time function, $x_c(t)$, in the time frame of $[-\tau/2; \tau/2]$ except for a region $[t_1; t_2]$, where it is constant, z (see Fig. 15). The function is continuous, differentiable and invertible outside of the constant part. The intensity density function can be derived from the cumulative distribution function (analogously to probability density function and probability distribution function):

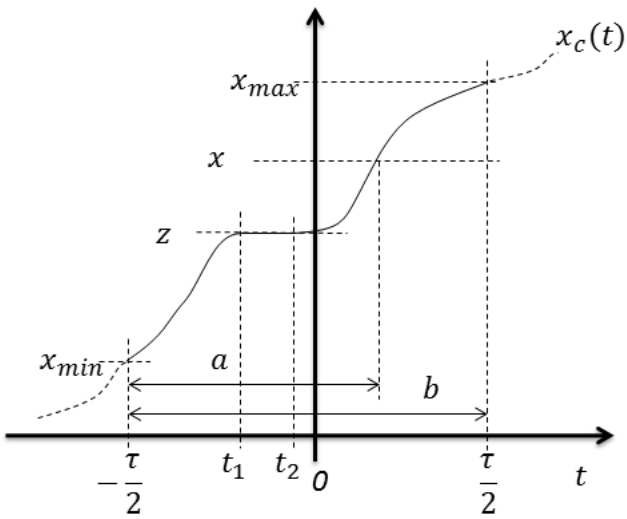

Fig. 15. Movement of marker center along *x* axis

For the above defined signal it becomes:

$$F(x) = P(\xi < x) = \frac{a}{b} = \begin{cases} 0, \quad if\ x < x_{min} \\ \dfrac{t(x) + \tau/2}{\tau}, \quad if\ x_{min} < x < z \\ \dfrac{t_1 + \tau/2}{\tau} + \dfrac{t_2 - t_1}{\tau}, \quad if\ z - 0 < x < z + 0 \\ \dfrac{t_1 + \tau/2}{\tau} + \dfrac{t_2 - t_1}{\tau} + \dfrac{t(x) - t_2}{\tau}, if\ z < x < x_{max} \\ 1, \quad if\ x \geq x_{max} \end{cases} \tag{18}$$

where $t(x)$ is the inverse function of $x_c(t)$. The intensity density function is derived from the cumulative distribution function by differentiation:

$$i(x) = \frac{dF(x)}{dx} = \begin{cases} \dfrac{1}{\tau}\dfrac{dt(x)}{dx} = \dfrac{1}{\tau}\dfrac{1}{\dfrac{dx_c(t)}{dt}} & if\ x \neq z \\ \dfrac{t_2 - t_1}{\tau}\delta(x) & if\ z - 0 < x < z + 0 \end{cases} \tag{19}$$

For strictly monotonic decreasing function we get:

$$F(x) = P(\xi < x) = \frac{\tau/2 - t(x)}{\tau} = \frac{1}{2} - \frac{t(x)}{\tau} \tag{20}$$

$$i(x) = \frac{dF(x)}{dx} = -\frac{1}{\tau}\frac{dt(x)}{dx} = -\frac{1}{\tau}\frac{1}{\frac{dx_c(t)}{dt}} \tag{21}$$

2) General continuous function

An arbitrary continuous function can be separated into segments. Each segment contains either a strictly monotonic increasing or decreasing or constant part. With the above separation the intensity of a pixel is the superposition of intensities of different segments. Let us introduce the following notation:

$$\begin{cases} S_{inc,k}: & k^{th} \text{ strictly mon. increasing segment of } x_c(t) \\ S_{const,l}: & l^{th} \text{ constant segment of } x_c(t) \\ S_{dec,m}: & m^{th} \text{ strictly mon. decreasing segment of } x_c(t) \end{cases} \qquad \begin{cases} X_{inc,k}: & \text{set of } x_c(t) \text{ belonging to } S_{inc,k} \\ X_{const,l}: & \text{set of } x_c(t) \text{ belonging to } S_{const,l} \\ X_{dec,m}: & \text{set of } x_c(t) \text{ belonging to } S_{dec,m} \end{cases}$$

$$\begin{cases} T_{inc,k}: & \text{set of } t \text{ belonging to } S_{inc,k} \\ T_{const,l}: & \text{set of } t \text{ belonging to } S_{const,l} \\ T_{dec,m}: & \text{set of } t \text{ belonging to } S_{dec,m} \end{cases} \qquad \begin{cases} i_{inc,k}(x): & \text{contribution of } S_{inc,k} \text{ to } i(x) \\ i_{const,l}(x): & \text{contribution of } S_{const,l} \text{ to } i(x) \text{ (Dirac delta!)} \\ i_{dec,m}(x): & \text{contribution of } S_{dec,m} \text{ to } i(x) \\ I_{const,l}(x): & \text{contribution of } S_{const,l} \text{ to } I(x) \end{cases}$$

$$F(x) = \begin{cases} 0 & if\ x < x_{min} \\ F_1(x) & if\ x_{min} < x < x_{max} \\ 1 & if\ x \geq x_{max} \end{cases} \tag{22}$$

$$\begin{aligned} F_1(x) = {} & \frac{1}{\tau}\sum_{x>X_{inc,k}} t_{dur,inc,k} + \frac{1}{\tau}\sum_{x>X_{const,l}} t_{dur,const,l} + \frac{1}{\tau}\sum_{x>X_{dec,m}} t_{dur,dec,m} \\ & + \frac{1}{\tau}\sum_{x\in X_{inc,k}} \left(t(x) - t_{start,inc,k}\right) + \frac{1}{\tau}\sum_{x\in X_{const,l}} t_{dur,const,l} \\ & + \frac{1}{\tau}\sum_{x\in X_{dec,m}} \left(t_{stop,dec,m} - t(x)\right) \end{aligned} \tag{23}$$

where $x > X_{inc,k}$ denotes that all elements of set $X_{inc,k}$ is smaller than x, $x > X_{dec,m}$ and $x > X_{const,l}$ similarly the same for $X_{dec,m}$ and $X_{const,l}$, $t_{dur,inc,k}$ denotes the duration of the segment $S_{inc,k}$, $t_{dur,dec,m}$ and $t_{dur,const,l}$ similarly, $t_{start,inc,k}$ denotes the start time of segment $S_{inc,k}$ and $t_{stop,dec,m}$ denotes the stop time

of segment $S_{dec,m}$. In the above equation $t(x)$ denotes the value corresponding to that particular segment. The intensity density function is obtained by differentiating the above eq. with respect to *x*:

$$i_1(x) = \frac{dF_1(x)}{dx} = \frac{1}{\tau}\sum_{x\in X_{const,l}} t_{dur,const,l}\delta\left(x\left(t \in T_{const,l}\right)\right) + \frac{1}{\tau}\sum_{x\in X_{inc,k}} \frac{dt(x)}{dx} - \frac{1}{\tau}\sum_{x\in X_{dec,m}} \frac{dt(x)}{dx}$$

$$= \frac{1}{\tau}\sum_{x\in X_{const,l}} t_{dur,const,l}\delta\left(x\left(t \in T_{const,l}\right)\right) + \frac{1}{\tau}\sum_{x\in X_{inc,k}} \frac{1}{\frac{dx_c(t)}{dt}} - \frac{1}{\tau}\sum_{x\in X_{dec,m}} \frac{1}{\frac{dx_c(t)}{dt}}$$

$$= \sum_{x\in X_{const,l}} i_{const,l}(x) + \sum_{x\in X_{inc,k}} i_{inc,k}(x) + \sum_{x\in X_{dec,m}} i_{dec,m}(x) \tag{24}$$

B. Geometric centroid as a function of time

Let us investigate the numerator of the geometric centroid expression, and substitute the coordinate *x* with its time dependent version. Different segments can have contribution to the intensity of the same pixel:

$$i(x) = \sum_k i_{inc,k}(x) + \sum_l i_{const,l}(x) + \sum_m i_{dec,m}(x) \tag{25}$$

Superposition of the segments can be written as:

$$\begin{aligned}\int_{x_{min}}^{x_{max}} x\, i(x)dx &= \sum_k \int_{x\in X_{inc,k}} x\, i_{inc,k}(x)dx + \sum_l \int_{x\in X_{const,l}} x\, i_{inc,l}(x)dx \\ &+ \sum_m \int_{x\in X_{dec,m}} x\, i_{dec,m}(x)dx \\ &= \sum_k \int_{t(x_{min})}^{t(x_{max})} x_c(t) i_{inc,k}\left(x_c(t)\right)\frac{dx_c(t)}{dt}dt + \sum_l x\left(t_{const,l}\right) I_{const,l}(x) \\ &- \sum_m \int_{t(x_{max})}^{t(x_{min})} x_c(t) i_{dec,m}\left(x_c(t)\right)\frac{dx_c(t)}{dt}dt\end{aligned} \tag{26}$$

Now let us combine the time dependent center point estimate with the time dependent intensity density function:

$$\int_{x_{min}}^{x_{max}} x\, i(x)dx = \underbrace{\sum_k \int_{t(x_{min})}^{t(x_{max})} x_c(t)\frac{1}{\tau}\frac{1}{\frac{dx_c(t)}{dt}}\frac{dx_c(t)}{dt}dt}_{\text{increasing segments}} + \underbrace{\sum_l x\left(t_{const,l}\right)\frac{1}{\tau}t_{dur,const,l}}_{\text{constant segments}}$$

$$+\underbrace{\sum_m \int_{t(x_{max})}^{t(x_{min})} x_c(t)\frac{1}{\tau}\frac{1}{\frac{dx_c(t)}{dt}}\frac{dx_c(t)}{dt}dt}_{\text{decreasing segments}} = \frac{1}{\tau}\int_{-\frac{\tau}{2}}^{\frac{\tau}{2}} x_c(t)dt \tag{27}$$

Summarizing the above derivation, for the center point estimate with normalized intensity we get:

$$x_{cog} = \frac{1}{\tau}\int_{-\tau/2}^{\tau/2} x_c(t)dt \tag{28}$$

or if the intensity is not normalized:

$$x_{cog} = \frac{\frac{1}{\tau}\int_{-\tau/2}^{\tau/2} x_c(t)dt}{\int_{x_{min}}^{x_{max}} i(x)dx} \tag{29}$$

which proves that geometric centroid based center point estimate can be well modeled with integral mean type distortion.

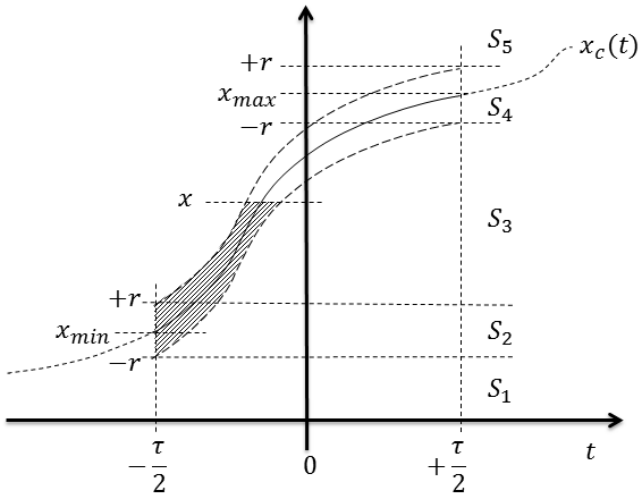

Fig. 16. Movement of the marker along the investigated scan line

APPENDIX 2 – MARKER WITH FINITE RADIUS

Let assume that the marker has a finite radius. The marker center moves along one axis according to a strictly monotonic, continuous, invertible time function in the time interval $[0; \tau]$. Radius of the marker (on the image) is R, width of the marker along the investigated scan line is $2r$ (Fig. 3). The center of the marker moves between x_{min} and x_{max}. Duration of the exposure is τ. Only one scan line will be investigated. The center point estimate is the average of estimates for all covered scan lines.

The intensity density function can be derived from the cumulative distribution function:

$$F(x) = P(\xi < x); \;\; i(x) = \frac{dF(x)}{dx} \tag{30}$$

The cumulative distribution is the shaded area compared to the area between +/-r curves (Fig. 16):

$$F(x) = \begin{cases} 0 & if\ S_1 \\ \frac{1}{2r\tau} \int_{-\tau/2}^{t(x+r)} x - (x_c(t) - r)dt & if\ S_2 \\ \frac{1}{2r\tau}\left(\int_{-\tau/2}^{t(x-r)} 2r\ dt + \int_{t(x-r)}^{t(x+r)} x - (x_c(t) - r)dt \right) & if\ S_3 \\ \frac{1}{2r\tau}\left(\int_{-\tau/2}^{t(x-r)} 2r\ dt + \int_{t(x-r)}^{\tau/2} x - (x_c(t) - r)dt \right) & if\ S_4 \\ 1 & if\ S_5 \end{cases}$$

$$\begin{cases} S_1 & if\ x \le x_{min} - r \\ S_2 & if\ x_{min} - r < x < x_{min} + r \\ S_3 & if\ x_{min} + r < x < x_{max} - r \\ S_4 & if\ x_{max} - r < x < x_{max} + r \\ S_5 & if\ x_{max} + r \le x \end{cases} \tag{31}$$

where $t(x)$ is the inverse function of the movement of marker center, $x_c(t)$. From this we get at different segments:

$$F(x, S_2) = \frac{1}{2r\tau}(x + r)\left(t(x + r) + \frac{\tau}{2}\right) - \frac{1}{2r\tau} \int_{-\tau/2}^{t(x+r)} x_c(t)dt \tag{32}$$

$$F(x, S_3) = \frac{1}{2r\tau} 2r\left(t(x - r) + \frac{\tau}{2}\right) + \frac{1}{2r\tau}(x + r)\big(t(x + r) - t(x - r)\big) - \frac{1}{2r\tau} \int_{t(x-r)}^{t(x+r)} x_c(t)dt \tag{33}$$

$$F(x, S_4) = \frac{1}{2r\tau} 2r\left(t(x - r) + \frac{\tau}{2}\right) + \frac{1}{2r\tau}(x + r)\big(\tau/2 - t(x - r)\big) - \frac{1}{2r\tau} \int_{t(x-r)}^{\tau/2} x_c(t)dt \tag{34}$$

Differentiating the above cumulative distribution function with respect to x we get the intensity density function:

$$i(x, S_1) = i(x, S_5) = 0 \tag{35}$$

$$i(x,S_2)=\frac{1}{2r\tau}\left(t(x+r)+\frac{\tau}{2}+(x+r)\left.\frac{dt}{dx}\right|_{x+r}\right)-\frac{1}{2r\tau}\frac{d}{dx}\int_{-\tau/2}^{t(x+r)}x_c(t)dt \tag{36}$$

$$\begin{aligned}i(x,S_3)=&\frac{1}{2r\tau}2r\left.\frac{dt}{dx}\right|_{x-r}+\frac{1}{2r\tau}\big(t(x+r)-t(x-r)\big)+\frac{1}{2r\tau}(x+r)\left(\left.\frac{dt}{dx}\right|_{x+r}-\left.\frac{dt}{dx}\right|_{x-r}\right)\\&-\frac{1}{2r\tau}\frac{d}{dx}\int_{t(x-r)}^{t(x+r)}x_c(t)dt\end{aligned} \tag{37}$$

$$\begin{aligned}i(x,S_4)=&\frac{1}{2r\tau}2r\left.\frac{dt}{dx}\right|_{x-r}+\frac{1}{2r\tau}\left(\frac{\tau}{2}-t(x-r)\right)+\frac{1}{2r\tau}(x+r)\left(-\left.\frac{dt}{dx}\right|_{x-r}\right)\\&-\frac{1}{2r\tau}\frac{d}{dx}\int_{t(x-r)}^{\tau/2}x_c(t)dt\end{aligned} \tag{38}$$

Using the Leibniz rule we can further simplify the above expressions:

$$\frac{\partial}{\partial x}\int_{t_a(x)}^{t_b(x)}x_c(t)dt=\int_{t_a(x)}^{t_b(x)}\frac{\partial}{\partial x}x_c(t)dt+x_c(t_b,x)\frac{\partial t_b(x)}{\partial x}-\ x_c(t_a,x)\frac{\partial t_a(x)}{\partial x} \tag{39}$$

As $x_c(t)$ does not depend on x, we get:

$$\frac{\partial}{\partial x}\int_{t_a(x)}^{t_b(x)}x_c(t)dt=x_c(t_b)\frac{\partial t_b(x)}{\partial x}-\ x_c(t_a)\frac{\partial t_a(x)}{\partial x} \tag{40}$$

$$i(x,S_2)=\frac{1}{2r\tau}\left(t(x+r)+\frac{\tau}{2}+(x+r)\left.\frac{dt}{dx}\right|_{x+r}\right)-\frac{1}{2r\tau}(x+r)\left.\frac{dt}{dx}\right|_{x+r}=\frac{1}{2r\tau}\left(t(x+r)+\frac{\tau}{2}\right) \tag{41}$$

$$\begin{aligned}i(x,S_3)=&\frac{1}{2r\tau}2r\left.\frac{dt}{dx}\right|_{x-r}+\frac{1}{2r\tau}\big(t(x+r)-t(x-r)\big)+\frac{1}{2r\tau}(x+r)\left(\left.\frac{dt}{dx}\right|_{x+r}-\left.\frac{dt}{dx}\right|_{x-r}\right)\\&-\frac{1}{2r\tau}(x+r)\left.\frac{dt}{dx}\right|_{x+r}+\frac{1}{2r\tau}(x-r)\left.\frac{dt}{dx}\right|_{x-r}=\frac{1}{2r\tau}\big(t(x+r)-t(x-r)\big)\end{aligned} \tag{42}$$

$$i(x,S_4)=\frac{1}{2r\tau}2r\frac{dt}{dx}\bigg|_{x-r}+\frac{1}{2r\tau}\left(\frac{\tau}{2}-t(x-r)\right)+\frac{1}{2r\tau}(x+r)\left(-\frac{dt}{dx}\bigg|_{x-r}\right)$$
$$-\frac{1}{2r\tau}(x-r)\left(-\frac{dt}{dx}\bigg|_{x-r}\right)=\frac{1}{2r\tau}\left(\frac{\tau}{2}-t(x-r)\right) \tag{43}$$

Summarizing the above we get the intensity density function along the investigated scan line:

$$i(x)=\begin{cases} 0 & if\ S_1 \\ \frac{1}{\tau}\cdot\frac{t(x+r)+\frac{\tau}{2}}{2r} & if\ S_2 \\ \frac{1}{\tau}\cdot\frac{t(x+r)-t(x-r)}{2r} & if\ S_3 \\ \frac{1}{\tau}\cdot\frac{\frac{\tau}{2}-t(x-r)}{2r} & if\ S_4 \\ 0 & if\ S_5 \end{cases} \tag{44}$$

If we compare it with (19) the major difference is that at final marker size finite difference replaces derivative. We can describe all regions on the same way if we introduce $t^*(x)$ as the extension of $t(x)$ at the borders:

$$t^*(x)=\begin{cases} -\frac{\tau}{2} & if\ S1\ or\ S_2 \\ t(x) & if\ S_3 \\ \frac{\tau}{2} & if\ S_4\ or\ S_5 \end{cases} \tag{45}$$

On that way intensity density function becomes:

$$i(x)=\frac{1}{\tau}\cdot\frac{t^*(x+r)-t^*(x-r)}{2r}\approx\frac{1}{\tau}\cdot\frac{dt^*(x)}{dx} \tag{46}$$

The center point estimate will be as close to the integral mean of the movement of marker center as close the above finite difference to the derivative is. From now on the derivation of the center point estimate is the same as for point like light sources. Thus, as long as the above approximation is valid, the distortion of the center point estimate can be described by integral mean type sampling model